GEOLOGICA CARPATHICA, APRIL 2007, 58, 2, 133–144

$^{40}Ar/^{39}Ar$ dating of detrital white mica of Upper Paleozoic sandstones in the Carnic Alps (Austria): implications for provenance and tectonic setting

DIETER MADER*, FRANZ NEUBAUER* and ROBERT HANDLER

Fachbereich Geographie und Geologie, Paris Lodron Universität Salzburg, Hellbrunnerstrasse 34, A-5020 Salzburg, Austria;
*✉ franz.neubauer@sbg.ac.at
*Present address: Department für Lithosphärenforschung, Universität Wien, Althanstraße 14, 1090 Wien, Austria; dieter.mader@univie.ac.at

(Manuscript received April 28, 2006; accepted in revised form October 5, 2006)

Abstract: New information on the geodynamic development and the provenance for Carboniferous to Permian successions exposed within the Carnic Alps is supplied by an integrated approach of microprobe analysis and $^{40}Ar/^{39}Ar$ dating of detrital white mica. $^{40}Ar/^{39}Ar$ analyses of detrital white mica concentrates (4–10 grains) from syn- and post-orogenic Mississippian to Late Permian successions display an apparently uniform population and time lag of the isotopic ages with respect to the stratigraphic age of their host rock: early Variscan ages (373–396 Ma) are reported within syn-orogenic Visean-Namurian turbiditic sandstones, Variscan ages (333–309 Ma) in post-orogenic Pennsylvanian and Permian terrestrial and shallow marine sandstones. Detrital white micas from Mississippian syn-orogenic sandstones indicate an intermediate time interval between the cooling of the source rock and deposition, typical for compressional accretionary wedge settings. Furthermore, these ages argue for a Middle Devonian tectonothermal event in the hinterland. Detrital white micas from Pennsylvanian sandstones indicate a very narrow time lag between post-Variscan cooling of the source region and the depositional age. This points to a rapid exhumation of rocks in the source region from mid-crustal levels prior to the deposition of these sediments.

Key words: Late Paleozoic, Southern Alps, Ar-Ar-dating, provenance, sandstones, detrital mica.

Introduction

The provenance and geodynamic development of sandstone successions can be classified by a variety of methods including petrographic analysis, whole rock and mineral chemistry and K-Ar and $^{40}Ar/^{39}Ar$ age dating (e.g. Hodges et al. 2005 and references therein).

Detrital white mica within clastic sediments originates from metamorphic or magmatic source rocks which were formed in middle levels of the continental crust. The K-Ar ages of these micas monitor the cooling of the crust of the hinterland below temperatures of about 350–410 °C, the approximate closure temperature of the argon isotopic system within white mica (Robbins 1972; Purdy & Jäger 1976; Hames & Bowring 1994; Kirschner et al. 1996), although the system is complicated by other factors (Villa 1998; McDougall & Harrison 1999 and references therein). The argon isotopic system of detrital white mica has been shown to be very resistant against mechanical and chemical weathering and sedimentary transport and is, therefore, very suitable for K-Ar and $^{40}Ar/^{39}Ar$ dating (e.g. Clauer 1981; Mitchell & Taka 1984).

Isotopic analyses may support stratigraphic and petrographic analyses for the identification of source areas of sediments and for the reconstruction of the paleogeographic and geodynamic evolution of sedimentary basins. K-Ar and $^{40}Ar/^{39}Ar$ isotopic analyses on detrital white mica for provenance and paleogeography of sedimentary basins include studies by Krylov & Silin (1959), Vistelius (1959), Fitch et al. (1966), Kelley & Bluck (1989, 1992), Dallmeyer (1987), Dallmeyer & Nance (1990), Renne et al. (1990), Welzel (1991), Dallmeyer & Takasu (1992), Aronson & Lewis (1994), Handler et al. (1997), and Sherlock et al. (2000). However, little attention has been paid to white micas from sedimentary basins of specific geodynamic settings. With the help of isotopic ages of detrital white mica, the exhumation rates of the continental crust can be calculated and indicators for the geodynamic situation are thus available (Copeland & Harrison 1990; Hodges et al. 2005). If the source rock reaches temperatures above the argon retention temperature of white mica, the K-Ar ages will become rejuvenated due to loss of radiogenic argon. Thus, the crustal rejuvenation rate indicates the extent of a young metamorphic overprint on continental crust (e.g. Neubauer & Handler 1997). The time interval between cooling of the source rock through the argon retention temperature and the time of deposition is a supporting method to classify various types of sedimentary basins.

The Carnic Alps have become a classical area for stratigraphic investigations of Paleozoic formations, due to the abundance of fossils, the structurally relatively undisturbed, although faulted, Upper Ordovician to Triassic sequences, and the very low-grade Variscan and Alpine metamorphic overprints (Schönlaub 1985a). In almost all lithostratigraphic sections of the Carnic Alps clastic sediments can be found at the base, and on the basis of ca. 640 Ma $^{40}Ar/^{39}Ar$ ages of detrital white mica, a Cadomian hinterland for Ordovician clastic sequences of the Carnic

Alps has been proposed (Dallmeyer & Neubauer 1994). Detrital white micas from other Paleozoic siliciclastic sequences of the Carnic Alps were not dated up to now.

We applied $^{40}Ar/^{39}Ar$ multigrain dating of detrital white mica from Carboniferous-Permian sequences to obtain radiometric ages and to evaluate current models for the geodynamic evolution of the Carnic Alps in conjunction with petrographic and geochemical data (Mader & Neubauer 2004). Contrasting $^{40}Ar/^{39}Ar$ ages of detrital white mica may indicate different provenances of detrital white mica within different types of Carboniferous-Permian sedimentary basins, such as a Mississippian syn-orogenic flysch trough and post-orogenic Pennsylvanian molasse basin of the Paleozoic of the Carnic Alps, as well as from the South-Alpine Permian passive continental margin. A high proportion of rejuvenated mica from continental hinterland crust, which was formed during the Variscan orogeny, may be detected by investigations of detrital white mica on Carboniferous syn-orogenic flysch and post-orogenic molasse sediments.

In addition, more information about the geodynamic development of the Paleozoic of the Carnic Alps should be obtained by $^{40}Ar/^{39}Ar$ dating of detrital white mica, because it would supply valuable information in conjunction with petrographic and geochemical data (Mader & Neubauer 2004).

Geological setting

The study area is located in the central Carnic Alps (Carinthia, Austria) on the Italian border (Figs. 1, 2). The Carnic Alps comprises the sedimentary basement of the Southern Alps, exposed in their north-eastern part, adjacent to and separated from the Austroalpine units by the Periadriatic fault (Fig. 1). Reviews on early research of this area can be found, for example in Schönlaub (1985a), Tollmann (1985) and Schönlaub & Histon (2000).

Together with the Graywacke Zone, and the southern Karawanken Alps, which both show some lithologic similarities and a similar general trend of sedimentary evolution to the Carnic Alps, and the Gurktal and Graz Paleozoic successions they are considered to be the southern external zone of the European Variscides, similar to the Rhenohercynic and Saxothuringic Zones, which represent the northern external zone (e.g. Schönlaub & Heinisch 1993).

The Carnic Alps are characterized by a continuous fossiliferous non- to low-grade metamorphosed sedimentary sequence reaching from the late Middle Ordovician to the early Pennsylvanian (with the Westphalian climax of the Variscan orogeny). They underwent deformation during both the Variscan and the Alpine orogeny. Evidence for Alpine tectonometamorphic activity is indicated by Cre-

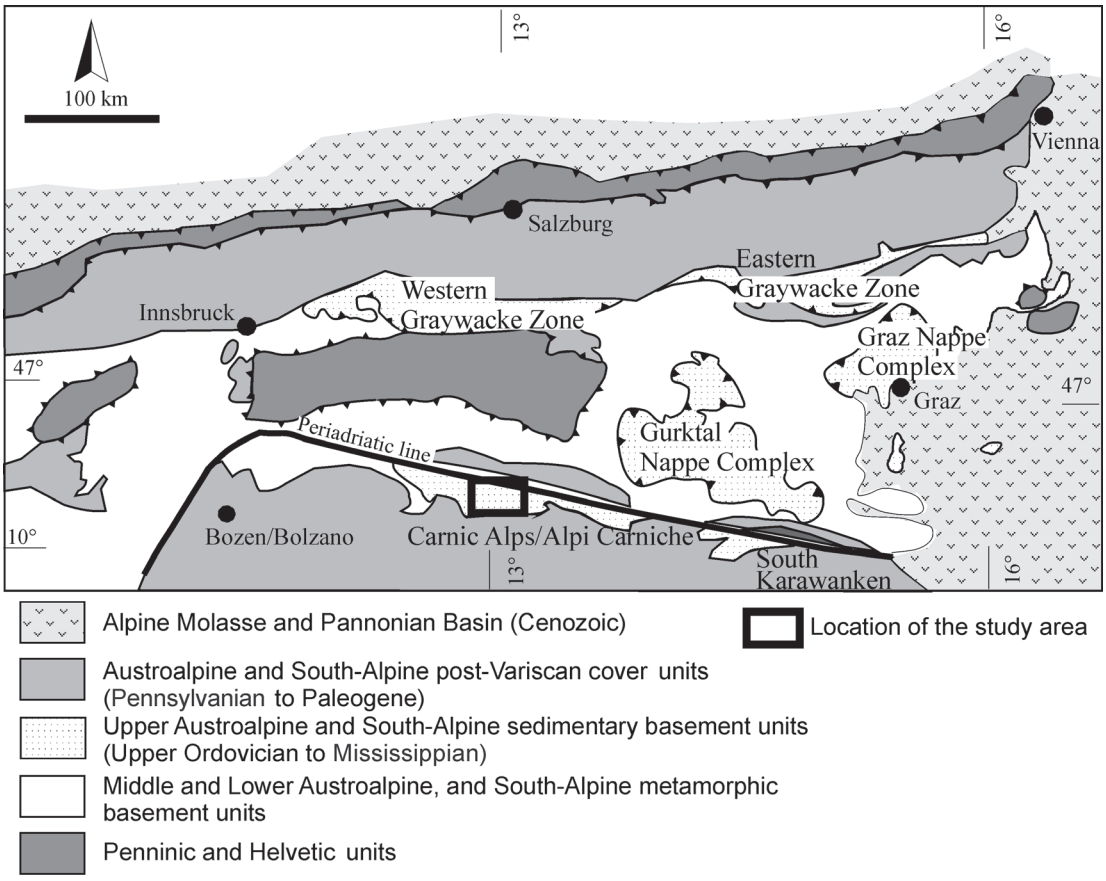

Fig. 1. Schematic geological map of Eastern and Southern Alps.

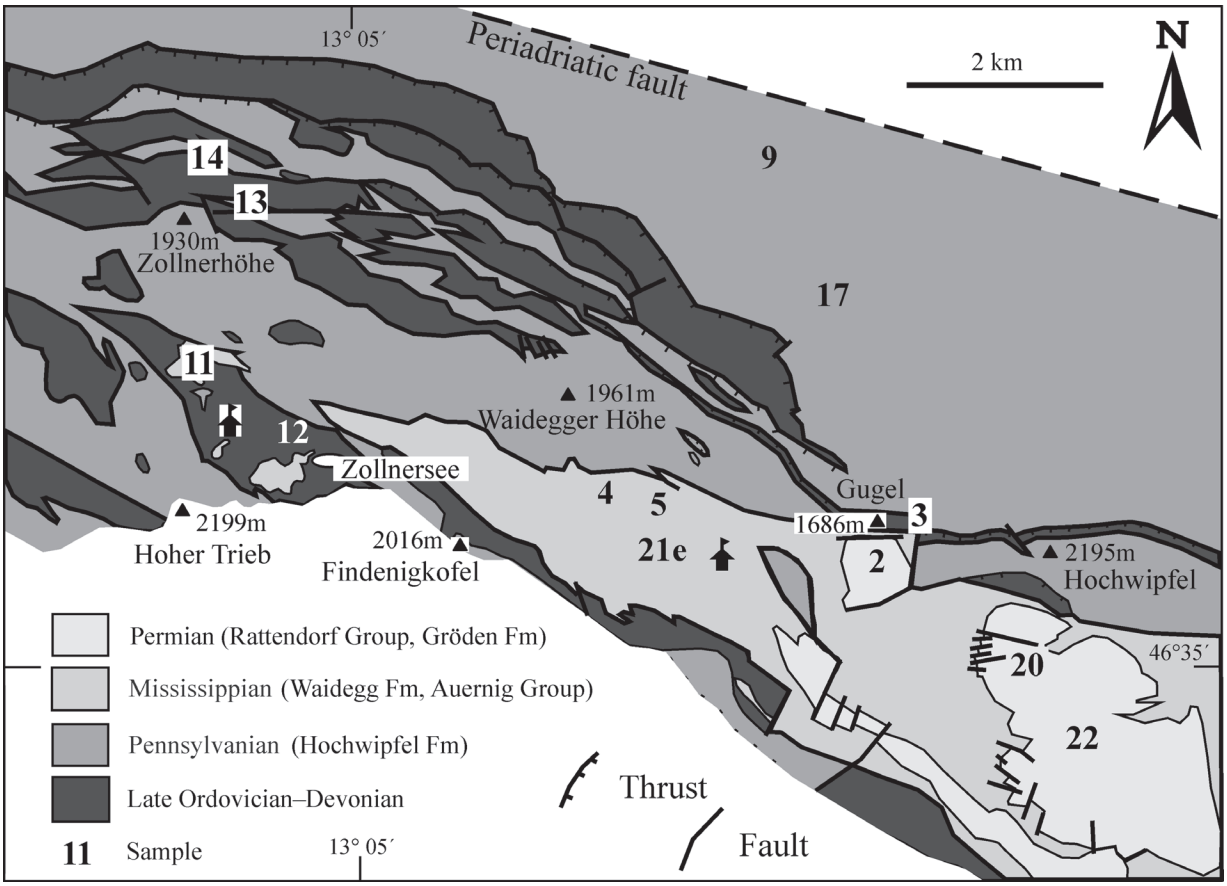

Fig. 2. Detailed map of the study area with sample locations (modified after Schönlaub 1985b, 1987). Sample 15 (from the Hochwipfel Formation) is located outside of the figure to the east.

taceous and Oligocene K-Ar ages from muscovite and illite from distinct blocks exposed along the Periadriatic Alps (Läufer 1996; Läufer et al. 1997). However, Alpine metamorphic conditions have not been sufficient to significantly overprint Variscan metamorphic fabrics and mineral assemblages (e.g. Rantitsch 1997; Läufer et al. 1997).

The stratigraphic sequence of the Carnic Alps can be divided into two major successions (Figs. 2, 3). These include a pre-orogenic sedimentary group, comprising Middle Ordovician to lowermost Pennsylvanian sequences, which are transgressively overlain by post-Variscan strata. These two successions are separated by an angular unconformity which formed at the Westphalian C/D boundary (e.g. Fenninger et al. 1976; Schönlaub 1985a; Schönlaub & Heinisch 1993 cum lit.).

The stratigraphic record starts with late Middle and Upper Ordovician siliciclastic and minor carbonate shallow-water deposits. These are overlain by Silurian to Lower Devonian black shales, thick platform carbonates, pelagic limestones, and siliciclastic sediments, which collectively indicate a basin-and-swell facies near a passive continental margin (Schönlaub & Histon 2000). From Late Devonian to Mississippian, pelagic limestones and lydites (cherts) occur, either suggesting enhanced subsidence and/or relative sea-level rise. The Visean-Namurian flysch

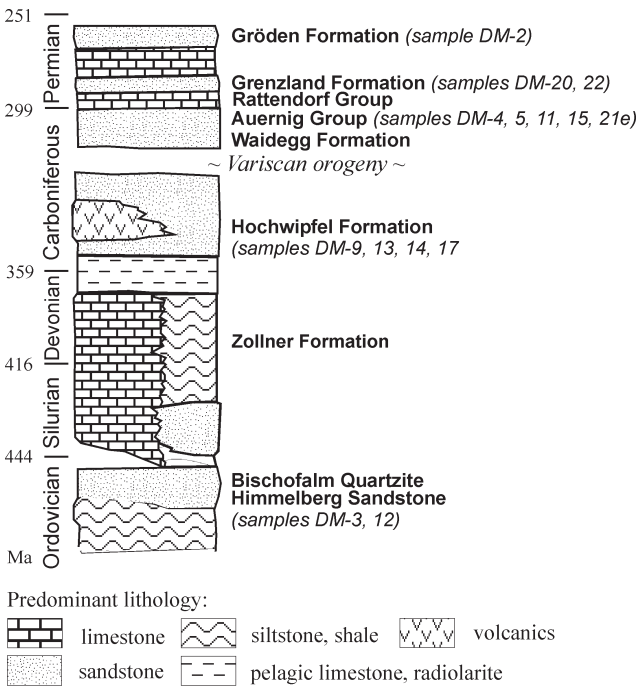

Fig. 3. Schematic stratigraphic section of the Paleozoic units in the Carnic Alps with emphasis on the siliciclastic sequences.

deposits with intercalations of olistoliths indicate the onset of the Variscan orogeny. From late Namurian to early Westphalian (Bashkirian to Moscovian) the Carnic Alps were uplifted and eroded for a period not longer than ca. 5 Myr (Flügel 1975; Spaletta et al. 1980).

Above a well-defined angular unconformity (Fenninger et al. 1976), Pennsylvanian molasse deposits (Auernig Group) occur. They grade into Lower Permian marine carbonates and Middle Permian siliciclastic red-beds and overlying Upper Permian shallow-marine carbonates of the South-Alpine Permian to Triassic succession (e.g. Krainer 1993 and references therein).

Samples were taken from Carboniferous to Permian sandstone-bearing formations in the central Carnic Alps (Fig. 2). On the basis of currently available geodynamic evidence (e.g. Schönlaub & Heinisch 1993; Neubauer & Sassi 1993; Krainer 1993; Schönlaub & Histon 2000; Läufer et al. 2001), previous (Dallmeyer & Neubauer 1994; Neubauer et al. 2001) and new samples, these were grouped into (1) Ordovician to Devonian extensional geodynamic environments (Himmelberg Sandstone, Bischofalm Quartzite, Zollner Formation), (2) Visean to Namurian (Mississippian to lowermost Pennsylvanian) contractional environments, as represented by syn-orogenic flysch formations (Hochwipfel Formation), (3) Pennsylvanian molasse (Waidegg/Malinifer Formation, Auernig Group), and (4) Permian extensional environments due to ongoing Alpine rifting (Grenzland Formation, Gröden Formation).

Analytical methods

White mica concentrates were prepared from sieve fraction 0.125–0.200 mm by flotation in water columns. Concentrates were cleaned in an ultrasonic bath with acetone, alcohol, and distilled water for 10 minutes each. Further purification was done by subsequent dry-sieving and separation by a Frantz isodynamic magnetic separator. Finally, mica grains were hand-selected under a binocular microscope.

The mineral concentrates for the $^{40}Ar/^{39}Ar$ dating were packed into high purity Al-sample holders and irradiated in the central position of the ASTRA reactor at the Austrian Research Centre in Seibersdorf, Austria for 1 to 3 hours. The flux within the reactor is 1.1×1014 n/cm^2 s. Correction factors for production of interfering isotopes have been reported by Frank et al. (1996) and are: $^{36}Ar/^{37}Ar(Ca)=0.0003$, $^{39}Ar/^{37}Ar(Ca)=0.00065$, and $^{40}Ar/^{39}Ar(K)=0.03$. Variations in the flux of neutrons were monitored with B4M white mica standard (Flisch 1982) for which a $^{40}Ar/^{39}Ar$ plateau age of 18.6±0.4 Ma has been reported (Burghele 1987). $^{40}Ar/^{39}Ar$ analyses were carried out in the ARGONAUT Laboratory at the Institute of Geology and Paleontology at the University of Salzburg using a UHV Ar-extraction line equipped with a combined MERCHANTEK^{TM} UV/IR laser ablation facility and a VG-ISOTECH^{TM} NG3600 Mass Spectrometer following procedures described in Handler et al. (2004). Stepwise heating analyses of samples are performed using a 25 W CO_2-IR laser operating in Tem_{00} mode at wavelengths between 10.57 and 10.63 µm. The laser is defocused to a spot size of ca. 1.0 mm. The laser is controlled from a PC, and the position of the laser beam on the sample is monitored through a double-vacuum window on the sample chamber via a video camera in the optical axis of the laser beam on a computer screen. Gas clean-up is performed using one hot and one cold Zr-Al SAES getter. Measurement is performed on an axial electron multiplier in static mode, peak-jumping of the magnet is controlled by a Hall-probe. For each gas increment the intensities of ^{36}Ar, ^{37}Ar, ^{38}Ar, ^{39}Ar and ^{40}Ar are measured, the baseline readings on mass 36.5 are subtracted. Intensities of the peaks are extrapolated over 16 measured intensities to the time of gas admittance into the mass spectrometer either by a straight line or a curved fit. Intensities are corrected for system blanks, background, post-irradiation decay of ^{37}Ar, and interfering isotopes. Ages and errors are calculated following suggestions by McDougall & Harrison (1999) and decay factors reported by Steiger & Jäger (1977).

Results

Composition of detrital mica

The results of electron microprobe analysis (reported in Mader & Neubauer 2004) were plotted in ternary diagrams (Fig. 4) with the compositional mol-percentage of muscovite, paragonite and aluminoceladonite (phengite of older literature) according to the recent nomenclature proposed by Rieder et al. (1998). We measured data both from thin sections and from magnetically separated concentrates. Interestingly, the magnetically separated grains show in general a lower percentage of aluminoceladonitic/phengitic micas. The reason is unknown.

The chemical composition of mica may reflect the nature of magmatic and metamorphic source rock (Speer 1984; Spear 1993). According to this the provenance from granites and regionally metamorphosed rocks may be indicated by mica compositions close to the muscovite corner. The more phengitic populations point to high-pressure metamorphic source rocks from deeper orogenic levels exposed by exhumation; high paragonite compositions (according to high sodium values) are interpreted as derivatives from low- to medium-grade metamorphic source rocks (Guidotti 1984 and references therein).

Late Ordovician sandstones display moderately phengitic micas in a thin section and more muscovite-rich micas in separate. Together, these data show some diversity of mica populations from this time slice.

The Visean-Namurian syn-orogenic samples may indicate two different sources (Fig. 4). Micas from specimen DM-9 plots near the muscovite-paragonite axis, whereas sample DM-14 demonstrates a more scattered pattern with a main spread along the muscovite-paragonite axis (Fig. 4). It should be noted, however, that, because of their scarcity, micas from the latter sample were not separated

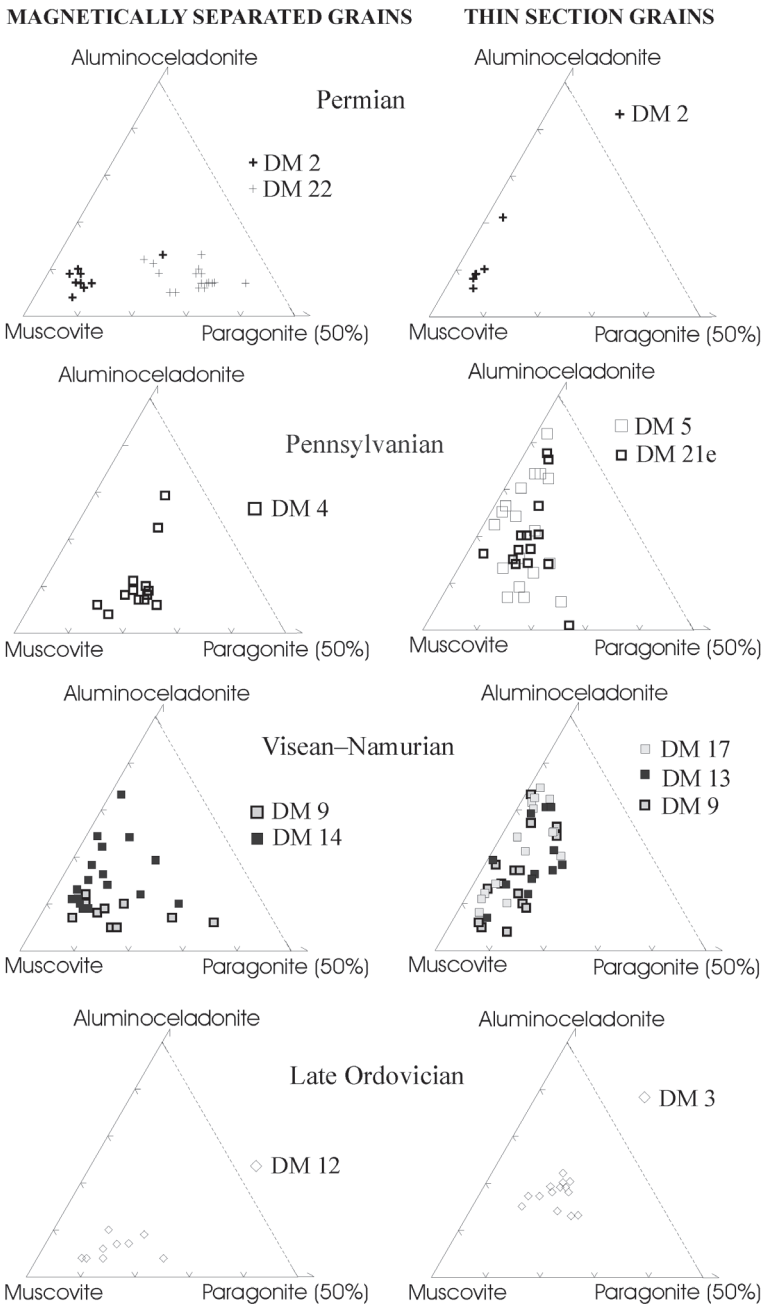

Fig. 4. Ternary plots showing the chemical variation of detrital white mica determined by electron microprobe. We apply the nomenclature proposed by Rieder et al. (1998). Results of magnetically separated micas of the grain size fraction 125–200 μm are shown. They illustrate the chemical variability of white mica within a sample. Because all micas analysed are primarily muscovite, the paragonite and aluminoceladonite corners were plotted at 50 %, whereby the latter indicate the composition of phengite.

with the highest magnetic susceptibility compared to the other samples. This may be the reason for their scattered plotting.

The multi-grain concentrate of the post-orogenic Pennsylvanian sample (DM-4) generally shows a narrower cluster of lower aluminoceladonitic (phengitic) but significantly higher paragonitic contents (Fig. 4). Two distinct mica populations may indicate two different sources.

The micas of the Early Permian sample (DM-22) show the highest paragonitic composition, whereas the phengitic component is generally not more than 20 % (Fig. 4). Low chemical diversity and a composition closely clustered to the muscovite corner are displayed by the Late Permian concentrate (DM-2).

$^{40}Ar/^{39}Ar$ data

The small grain size did not allow good single grain analyses. So, 4 to 10 grains per sample were selected to get a first order approximation of age populations. Fortunately, this approach yielded reasonably good results and revealed a first order distinction of age populations from time level to time level. Analytical results are listed in Table 1 and are portrayed as age spectra in Fig. 5. The small increments throughout the release spectra with highly variable ages are not interpreted as reflections of disturbed argon isotopic systems of the white micas analysed. However, possible mixtures of muscovite, aluminoceladonite/phengite and paragonite in the concentrate analysed (4–10 white micas) cannot be excluded and may be reflected by the disturbed age spectra. Muscovite has a lower closure temperature compared to aluminoceladonite/phengite and paragonite (e.g. von Blanckenburg et al. 1989; McDougall & Harrison 1999), which will result in unstable age spectra. Furthermore, weak, very low-grade Carboniferous and Cretaceous/Oligocene metamorphic overprints have been reported from Carboniferous rocks of the working area adjacent to the Periadriatic fault (Läufer et al. 1997, 2001). A tectonometamorphic event, with K-Ar ages of illite of 300–320 Ma, is reported for the Hochwipfel Nappe in Läufer et al. (2001), which may also have slightly affected the K/Ar isotopic system. This resulted in some minor Ar loss in low-temperature increments of some samples (see below).

Sample DM-2 (Gröden Formation; Late Permian) displays a discordant age pattern with an apparent age of 319.7±3.4 Ma for the largest increment (53.5 % of total ^{39}Ar released) which is similar within the error to the total gas age of 319.2±4.7 Ma. We suggest therefore, that this age is geologically significant, and may be interpreted as the average age of cooling through the appropriate argon retention temperature after peak conditions of metamorphic/plutonic temperature conditions at ca. the Mississippian to Pennsylvanian boundary.

Both Early Permian samples display rather concordant patterns. Sample DM-20 (Grenzland Formation) yielded an apparent age of 334.4±2.6 Ma for the largest increment

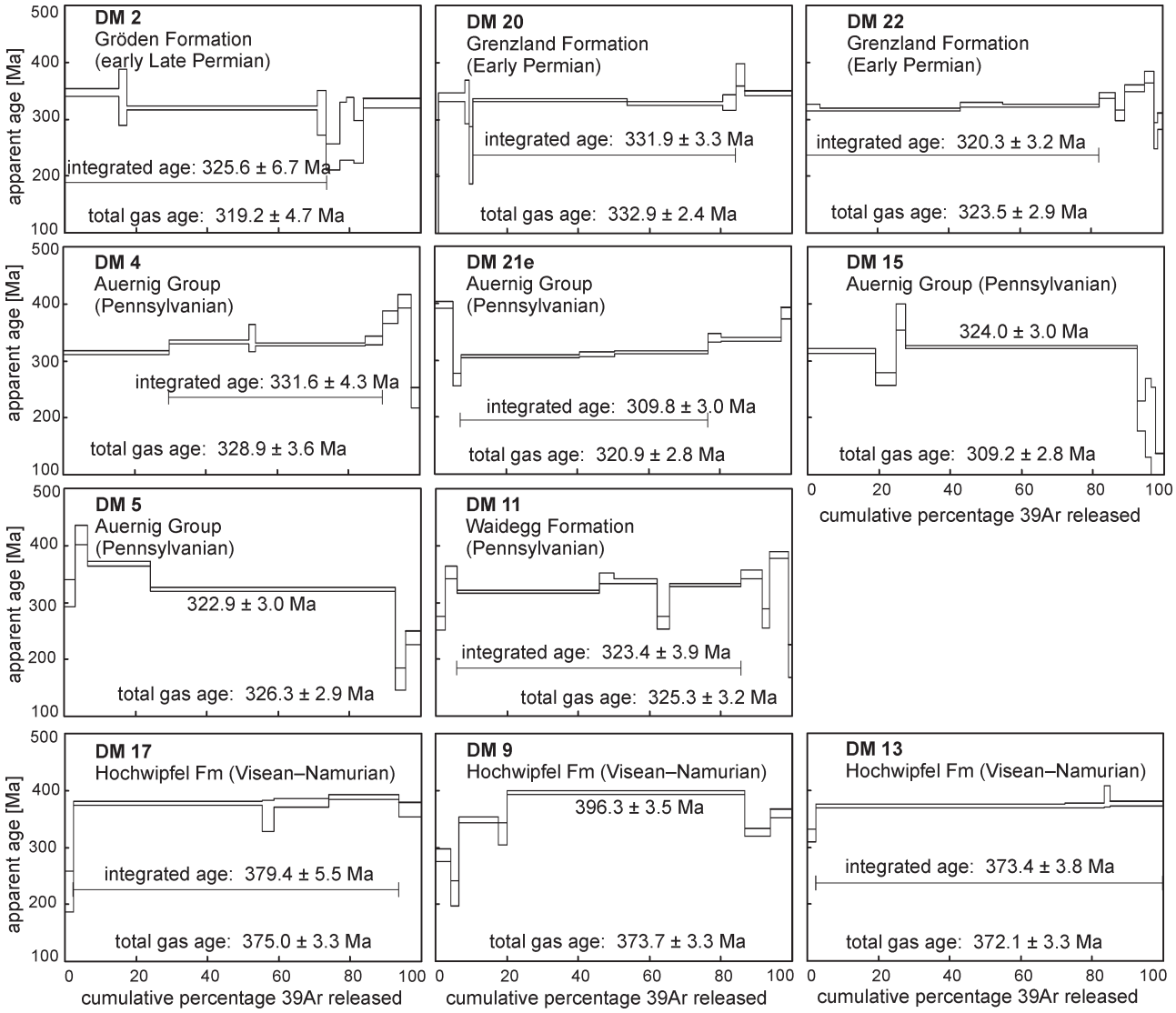

Fig. 5. Apparent $^{40}Ar/^{39}Ar$ age spectra of detrital white mica. Experimental laser energy output increases from left to right. Width of the bar corresponds to the analytical 2σ error.

(43.1 % of total ^{39}Ar released) and total gas age of 332.9±2.4 Ma. In sample DM-22 (Grenzland Formation) an apparent age of 316.5±2.8 Ma is indicated by the largest increment (39.2 % of total ^{39}Ar released, a total gas age 320.3±3.2 Ma and an integrated age of 323.5±2.9 Ma (Fig. 5).

Similar results are indicated by the Pennsylvanian samples of the Auernig Group and Waidegg Formation with total gas ages ranging between 309.2±2.8 to 328.9±3.6 Ma (Table 1). The largest increment of sample DM-15 (64.8 % of total ^{39}Ar released) and sample DM-5 (68.8 % of total ^{39}Ar released) yielded apparent ages of 324.0±3.0 Ma and 322.9±3.0 Ma respectively. Sample DM-21e yielded an apparent age of 320.9±2.8 Ma. An apparent age of 309.8±3.0 Ma is indicated by three internally concordant steps, together comprising 69.2 % of total ^{39}Ar released, which is interpreted as being geologically significant. The first and last steps show an older age component 396.7±6.2 and 381.9±10 Ma which suggests the presence of an older age group and, therefore, an inhomogeneous age composition of the sample. A component with a similar age of 404±12 Ma is indicated by step 7 of sample DM-4. The largest increment of sample DM-11 from the Pennsylvanian Waidegg Formation yielded an apparent age of 318.6±2.9 Ma (40.0 % of total ^{39}Ar released) which is again relatively close to the total gas age of 325.3±3.2 Ma.

Detrital white micas of the Mississippian Hochwipfel Formation yield total gas ages between 372.1±3.3 and 375.0±3.3 Ma (Table 1). Sample DM-9 displays a staircase increase of ages from minimum 219.4±22.5 Ma to the largest increment with an apparent age of 396.3±3.5 Ma (66.6 % of total ^{39}Ar released). Similarly, samples 13 and 17 show a lower age in the first increments with ages of 320±11 and 222±36 Ma, respectively. An apparent age of 379.5±8.2 Ma is recorded by the increment 2–5 with 92.3 % ^{39}Ar released in sample DM-17. Detrital white mi-

Table 1: Ar-analytical data from multi-grain incremental heating analysis on detrital muscovite from the Carnic Alps, Austria. Errors are 1-sigma inter-laboratory. *Continued on the next page.*

Increment	$^{36}Ar/^{39}Ar^{a}$	$^{37}Ar/^{39}Ar^{b}$	$^{40}Ar/^{39}Ar^{a}$	$\%^{39}Ar$	$\%^{40}Ar^{c}$	age	+/–
DM-2 (Gröden Formation. Late Permian), J-Value: 0.001181 ± 0.000012							
1	0.0834	0.76	204.1	15.23	87.92	347.0	7.1
2	0.1821	43.71	219.7	2.22	75.50	338.4	49.4
3	0.0130	1.65	167.7	53.50	97.72	319.7	3.4
4	0.0669	52.82	169.0	2.30	88.30	311.0	39.5
5	0.1284	41.01	148.3	3.90	74.41	233.7	23.2
6	0.0975	87.09	154.4	1.99	81.34	278.4	51.6
7	0.3346	60.64	231.6	2.07	57.31	282.9	55.8
8	0.2245	49.48	189.1	2.60	64.93	260.2	37.5
9	0.0909	11.79	193.1	16.17	86.09	327.6	8.5
Total	0.0597	10.97	179.4	100.00	90.17	319.2	4.7
DM-4 (Auernig Group, Late Carboniferous), J-Value: 0.001181 ± 0.000012							
1	0.0200	1.64	167.0	29.72	96.46	314.8	2.9
2	0.0077	3.59	173.7	22.29	98.69	333.9	3.5
3	0.13323	48.66	205.3	1.87	80.83	340.3	23.4
4	0.0120	3.16	172.3	30.83	97.94	329.0	3.2
5	0.0562	11.67	187.2	4.93	91.14	335.3	7.6
6	0.0649	24.22	210.5	4.31	90.89	376.6	11.5
7	0.0592	20.58	225.5	3.57	92.24	404.2	11.9
8	0.1308	41.60	150.0	2.47	74.23	235.7	17.4
Total	0.0248	6.56	175.4	100.00	95.83	328.9	3.6
Steps 2 – 5				59.92		331.6	4.3
DM-5 (Auernig Group, Late Carboniferous), J-Value: 0.003787 ± 0.000038							
1	0.1706	0.8171	100.81	3.05	49.98	315.5	23.9
2	0.1484	0.3064	112.82	3.53	61.13	418.7	17.3
3	0.0028	0.0534	60.59	17.52	98.62	367.9	4.7
4	0.0065	0.0087	53.71	68.78	96.41	322.9	3.0
5	0.2296	0.7920	93.05	2.89	27.10	164.9	19.4
6	0.1333	0.1358	76.69	4.22	48.65	238.4	12.0
Total	0.0277	0.0799	60.54	100.00	86.49	326.3	2.9
DM-9 (Hochwipfel Formation, Visean-Namurian), J-Value: 0.003787 ± 0.000038							
1	0.1413	0.0061	87.16	4.38	52.08	286.0	11.3
2	0.2614	0.1375	111.40	2.14	30.66	219.4	22.5
3	0.0333	0.0953	66.09	11.04	85.12	348.3	5.0
4	0.1307	1.3142	90.44	2.57	57.30	324.0	19.3
5	0.0032	0.0390	65.83	66.57	98.58	396.3	3.5
6	0.0180	0.2697	57.63	7.19	90.77	326.1	6.9
7	0.0009	0.2049	58.63	6.12	99.53	360.2	7.4
Total	0.0223	0.1054	67.37	100.00	90.23	373.7	3.3
DM-11 (Waidegg Formation, Late Carboniferous), J-Value: 0.001181 ± 0.000012							
1	0.1195	11.09	166.7	2.57	78.82	263.8	12.0
2	0.0287	17.97	187.6	3.28	95.48	352.6	11.6
3	0.0111	0.19	166.8	40.01	98.03	318.6	2.9
4	0.0785	12.34	197.8	4.17	88.27	342.5	9.3
5	0.0310	5.94	182.6	11.99	94.98	338.2	4.3
6	0.0962	20.76	158.6	3.54	82.08	264.7	11.5
7	0.0237	0.84	177.1	20.16	96.05	330.5	3.2
8	0.0544	10.70	194.6	5.90	91.74	349.1	7.6
9	0.1403	26.58	174.6	2.03	76.25	272.0	16.6
10	0.0263	4.37	207.3	5.27	96.25	383.4	6.5
11	0.2785	6.49	179.0	1.08	54.02	196.9	28.6
Total	0.0341	4.55	176.5	100.00	94.29	325.3	3.2
DM-13 (Hochwipfel Formation, Visean-Namurian, J-Value: 0.003787 ± 0.000038							
1	0.0281	0.0097	59.56	2.45	86.08	320.0	11.0
2	0.0018	0.0009	61.09	69.94	99.11	372.2	3.3
3	0.0090	0.0606	63.42	11.05	95.79	373.4	4.2
4	0.0208	0.3840	69.67	1.60	91.22	389.2	19.1
5	0.0065	0.0560	63.28	14.96	96.97	376.8	4.1
Total	0.0043	0.0221	61.77	100.00	97.95	372.1	3.3
Steps 2–5				97.55		373.4	3.8

Table 1: *Continuation from the previous page.*

Increment	$^{36}Ar/^{39}Ar^{a}$	$^{37}Ar/^{39}Ar^{b}$	$^{40}Ar/^{39}Ar^{a}$	$\%^{39}Ar$	$\%^{40}Ar^{c}$	age	+/–
DM-15 (Auernig Group, Late Carboniferous), J-Value: 0.003787 ± 0.000038							
1	0.0220	0.0193	57.23	19.15	88.64	316.9	3.9
2	0.0839	0.1822	67.08	5.69	63.06	268.0	10.8
3	0.3236	0.2896	157.04	2.70	39.11	377.3	23.0
4	0.0102	0.0075	54.98	64.84	94.52	324.0	3.0
5	0.0894	0.3683	57.89	2.24	54.36	203.2	26.8
6	0.9778	0.6241	319.75	1.70	9.63	199.3	69.1
7	1.0126	0.5516	323.63	1.23	7.54	159.7	93.1
8	0.3997	0.4037	133.81	2.44	11.73	104.2	33.3
Total	0.0652	0.0622	68.66	100.00	71.94	309.2	2.8
DM-17 (Hochwipfel Formation, Visean-Namurian), J-Value: 0.003787 ± 0.000038							
1	0.0117	0.3706	38.08	2.36	90.94	222.4	36.0
2	0.0029	0.0137	62.37	53.03	98.62	377.6	4.0
3	0.0231	0.1186	64.34	3.14	89.39	355.4	26.7
4	0.0344	0.0572	71.83	15.43	85.85	378.5	7.1
5	0.0113	0.0255	66.82	19.68	95.01	388.5	4.8
6	0.0024	0.0158	60.11	6.36	98.83	365.9	12.6
Total	0.0102	0.0347	64.05	100.00	95.28	375.0	3.3
Steps 3–6				44.61		379.5	8.2
DM-20 (Grenzland Formation, Early Permian), J-Value: 0.003787 ± 0.000038							
1	0.3472	1.2254	120.89	0.74	15.15	121.6	81.8
2	0.0362	0.0934	65.34	7.39	83.65	339.3	7.6
3	0.1387	0.3717	94.18	1.34	56.49	331.2	38.3
4	0.0577	1.1255	54.01	1.04	68.45	237.0	49.8
5	0.0000	0.0038	53.82	43.12	99.98	334.4	2.6
6	0.0016	0.0320	53.19	26.86	99.12	328.3	3.0
7	0.0186	0.0628	58.39	3.80	90.57	329.2	13.4
8	0.0033	0.0226	62.73	2.40	98.45	379.0	19.7
9	0.0020	0.0555	56.29	13.31	98.97	345.2	4.2
Total	0.0092	0.0534	56.26	100.00	95.17	332.9	2.4
DM-21e (Auernig Group, Late Carboniferous), J-Value: 0.001181 ± 0.000012							
1	0.0830	2.538	232.26	5.13	89.44	396.7	6.2
2	0.2121	8.155	195.73	2.33	67.98	265.9	11.6
3	0.0113	0.400	160.16	33.20	97.91	306.6	2.8
4	0.0464	2.762	172.18	9.71	92.03	310.4	4.0
5	0.0241	0.903	167.72	26.25	95.75	313.6	2.9
6	0.0637	3.672	193.43	3.78	90.27	339.5	7.4
7	0.0203	1.120	179.21	16.81	96.66	336.1	3.2
8	0.1281	10.688	235.17	2.78	83.91	381.9	10.1
Total	0.0332	1.583	174.39	100.00	94.38	320.9	2.8
DM-22 (Grenzland Formation, Early Permian), J-Value: 0.001181 ± 0.000012							
1	0.1654	2.853	212.9	3.99	77.05	320.5	6.5
2	0.0038	0.797	163.4	39.21	99.32	316.5	2.8
3	0.0109	5.366	169.7	11.84	98.10	325.6	3.8
4	0.0053	1.101	167.7	27.06	99.06	323.5	2.9
5	0.0404	0.166	188.4	4.54	93.67	341.5	5.7
6	0.0226	7.829	162.0	2.73	95.89	306.6	8.9
7	0.0016	6.024	183.3	5.56	99.74	354.8	5.7
8	0.0098	7.355	196.5	2.70	98.52	374.1	10.6
9	0.2283	12.992	202.2	0.96	66.64	270.6	23.0
10	0.0655	20.847	167.2	1.42	88.42	297.3	14.6
Total	0.0167	2.535	170.8	100.00	97.10	323.5	2.9

[a] measured
[b] corrected for post-irradiation decay of ^{37}Ar (35.1 days half-life)
[c] $(^{40}Ar_{tot} - {}^{36}Ar_{atmos} \times 295.5) / {}^{40}Ar_{tot}$

cas of sample DM-13 yielded an apparent age of 372.1±3.3 Ma (70.0 % of total ^{39}Ar released of the largest increment with an age of 372.2±3.3). We interpret lower ages in the low-temperature increments of all three samples of the Hochwipfel Formation to result from Ar loss during a weak Cretaceous/Oligocene metamorphic overprint as these samples are close to the Periadriatic fault where Rantitsch (1997) and Läufer et al. (1997) reported a very-low grade metamorphic overprint. We interpret the integrated ages of samples DM-13 and 17 and the large gas volume steps age of sample DM-9 to be geologically significant and to represent the average age of cooling through the appropriate argon retention temperature in the source region.

Together, the ages show clearly two age groups although the ages are variable within these groups: (1) an age of 373.4±3.8 to 396.3±3.5 Ma in the Hochwipfel Formation (Visean to Namurian), and (2) an age group ranging from 309.8±3.0 to 331.9±3.3 Ma for post-Variscan Waidegg to Gröden Formations (Pennsylvanian to early Late Permian).

Discussion

Our new $^{40}Ar/^{39}Ar$ data from Upper Paleozoic sandstones of the Carnic Alps have significance both for the Paleozoic evolution of the Carnic Alps and the basement evolution of the Alps as a whole. We discuss first the chemical variation of investigated micas and, then age data with the main goal of putting all data in a sequence of geodynamic models to explain our new data in the context of the available literature. These models are shown in Fig. 6.

The low chemical diversity of the micas within individual samples indicates rather homogeneous source areas for each lithostratigraphic unit except the Carboniferous micas display a more diverse chemical composition, both within each sample and between the individual samples (Mader & Neubauer 2004). Hence, distinct source regions can be assumed for these samples. The relatively homogeneous chemical compositions indicate a rather limited possibility for mixture of different source rocks within each sample. This is an important fact regarding the multi-grain radiometric age determination of detrital white mica.

A trend from fairly aluminoceladonitic/phengitic composition (Carboniferous) to muscovitic-paragonitic micas (Permian) is indicated. The composition of the Visean–Namurian Hochwipfel Formation is explained as representing magmatic and high-grade metamorphic sources of the just uplifted, exhumed and denuded Variscan orogen. The rather large spread of these data may be interpreted as an indication of diversity in source regions. In the Pennsylvanian, post-orogenic sediment material was likely derived from high-pressure dominated metamorphic rocks as seen in the high aluminoceladonitic/phengitic components, but without significant magmatic supply.

Undisturbed integrated ages and ages represented by the large gas volumes are interpreted as cooling ages of the detrital white micas in the respective source areas. The interval between apparent cooling age of white mica (closure temperature ca. 350–410 °C, e.g. von Blanckenburg et al. 1989) and depositional biostratigraphic age of post-orogenic rocks can be used as a measure for the exhumation rate in the source region (Copeland & Harrison 1990; Hodges et al. 2005 and references therein). This represents the exhumation of the continental crust from the depth of closing temperature, which is assumed as middle-upper crust (ca.

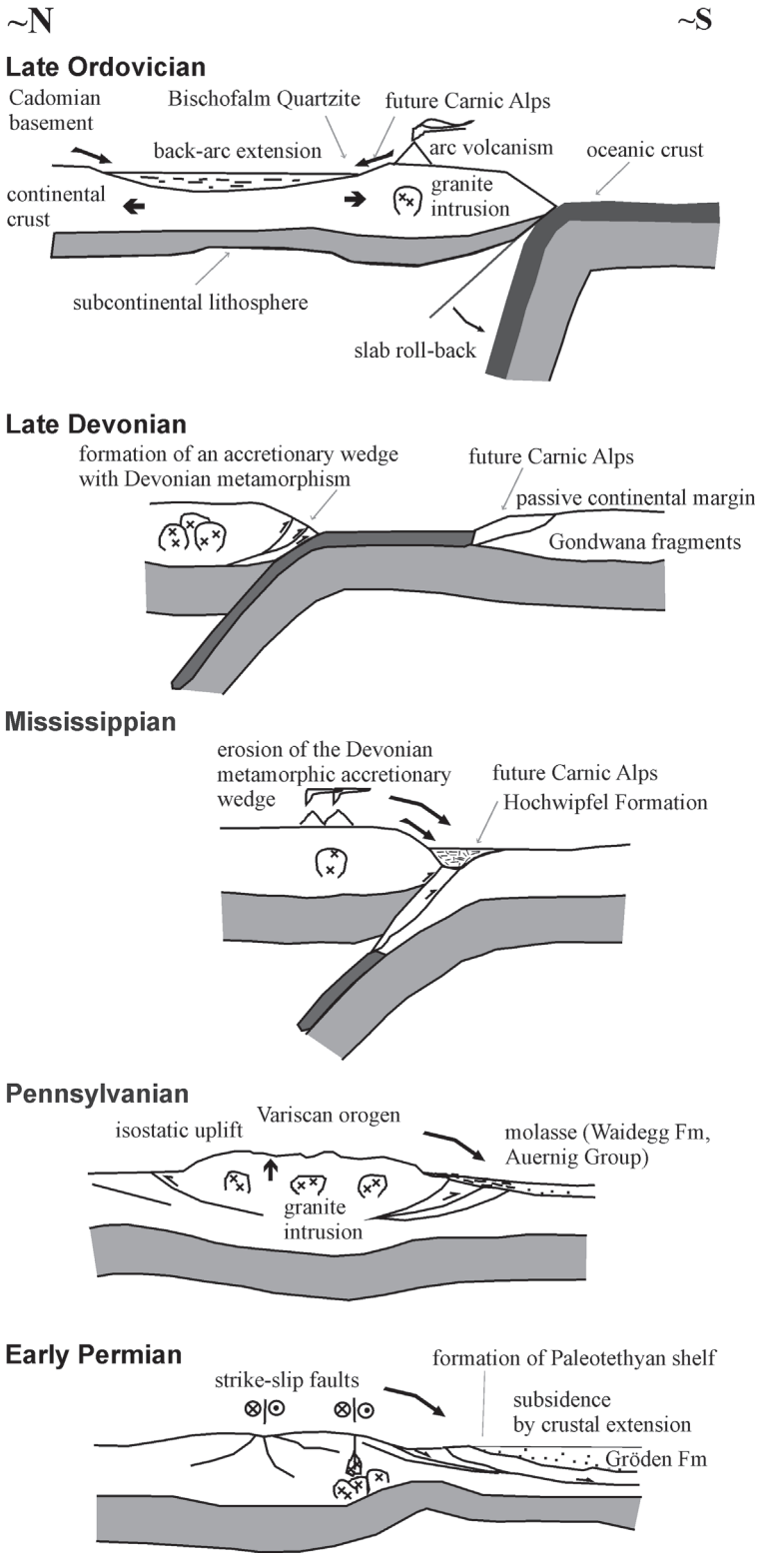

Fig. 6. Late Ordovician to Late Permian tectonic evolution of the Carnic Alps.

10–15 km depth, at a normal geothermal gradient), to the erodable surface (e.g. Neubauer & Handler 1997).

Previously reported $^{40}Ar/^{39}Ar$ white mica and U-Pb zircon ages argue for a Cadomian source of clastic material in the Late Ordovician (Dallmeyer & Neubauer 1994; Neubauer et al. 2001), tentatively back-arc extensional setting of the Carnic Alps (Fig. 6).

The white micas from Visean–Namurian samples may have undergone an early Variscan tectonothermal event. In general, only a very weak tectonothermal overprint during Late Paleozoic Variscan orogenic events is recognized in the Carnic Alps. Low-temperature increments of micas from the Hochwipfel Formation display apparent ages of 286±11 Ma, 320±11 Ma, and 222±36 Ma, which can be interpreted as reflecting minor rejuvenation during Alpine orogenic events. The similar Middle Devonian ages for Visean–Namurian samples may be attributed to a fairly homogeneous source region, which is also indicated by geochemical analysis (Mader & Neubauer 2004). The Devonian metamorphosed Austroalpine crystalline complex was postulated as a possible source for these flysch deposits (Neubauer 1988) (Fig. 6). Similar Middle Devonian $^{40}Ar/^{39}Ar$ ages have been recently reported from two Austroalpine units, the Kaintaleck Metamorphic Complex of the Eastern Graywacke Zone (Handler et al. 1999) and the Wechsel Gneiss Complex (Müller et al. 1999). Similar Devonian ages by Pb-Pb zircon evaporation were reported from the Hochwipfel Formation of the South Karawanken (Sonntag et al. 1997) exposed towards the east of the Carnic Alps, which supports the significance of this age group. Their Pb-Pb ages are explained as records of the magmatic rocks in the source region. Interestingly, Vozárová et al. (2005) recently reported similar early Variscan multi-grain $^{40}Ar/^{39}Ar$ ages of white mica from Westphalian sandstones and conglomerates from the Rudňany Formation of Western Carpathians.

The post-Variscan detrital micas of the Auernig sandstones record relatively rapid exhumation according to apparent cooling ages between ca. 309.8±3.0 Ma and 331.9±3.3 Ma (Fig. 5). Hardly any record is present of older sources. This suggests that nearly the entire upper crust, above the Ar retention temperature of ca. 350–410 ºC was removed prior to deposition of post-Variscan molasse. This is entirely different from the Alpine molasses where only a low percentage of young micas is recorded (e.g. von Eynatten et al. 1999) and also dissimilar to the Himalaya orogen with a fairly low but still recognizable percentage of old micas (e.g. Najman et al. 2001). Also for similarly aged clastic successions, Vozárová et al. (2005) recently reported the same Variscan multi-grain $^{40}Ar/^{39}Ar$ ages of white mica from the Western Carpathians.

The relationships between cooling and depositional ages suggest that the exhumation of these rocks occurred in about 2–25 Myr or max. 39 Myr (using time intervals of 311 to 290 Ma, after Gradstein et al. 2004, for the depositional range of the post-Variscan sediments). The apparent ages of the post-Variscan overstep sequences are interpreted as post-metamorphic cooling ages of the deeply buried source rocks recording approximately the minimum age of the Variscan orogenic phase. The uncertainty of stratigraphy of the Auernig Formation does not allow a more detailed correlation between cooling in the source region and sediment deposition. Detrital white micas from the Permian Gröden- and Grenzland Formations demonstrate ages similar to the earliest post-orogenic sandstones of the Waidegg Formation and Auernig Group. This suggests that erosion affected similar tectonic horizons as during Pennsylvanian times (Fig. 6).

It should be noted that nearly no Alpine tectonothermal overprint is reflected in the apparent ages of both the syn- and post-orogenic Upper Paleozoic samples. This indicates weak Alpine metamorphic conditions in the realm of the Carnic Alps, not exceeding 250–300 ºC in accordance with previous observations (Rantitsch 1997; Läufer et al. 1997, 2001).

According to Neubauer & Handler (1997), variations in residence time intervals between the closure temperature and depositional age may bear on the geodynamic setting of sedimentary basins. The new radiometric data suggest the following sequence of events, using time calibration data after Gradstein et al. (2004): The white micas of the Middle Permian Gröden Formation display a lag time/residence interval of about 60–70 Myr, reflecting an extensional setting with deeply eroded source regions. Post-orogenic Pennsylvanian sandstones show very low residence intervals (ca. 2–39 Myr), reflecting the geodynamic setting of a peripheral molasse/intramontane basin adjacent to a rapidly rising orogen. A residence time interval of ca. 30–70 Myr is demonstrated by the detrital white micas of the Hochwipfel Formation. Since no rejuvenated mica occur because of insufficient Variscan tectonothermal overprint a higher residence time interval is shown than expected for a syn-collisional flysch basin, which should contain material both from older basement and from younger sedimentary cover sequences of the overridden plate.

Conclusions

Microprobe data of detrital white mica not only supply information regarding their variable chemical composition, important for the interpretation of their distinct closing temperatures, but can also supply arguments concerning the provenance of the detrital micas. $^{40}Ar/^{39}Ar$ data of detrital white mica from Visean–Namurian sandstones (Hochwipfel Formation) of the Carnic Alps record early Variscan ages (373.4±3.8 to 396.3±3.5 Ma) in the white mica demonstrating an undetectable to low thermal effect of both the Variscan and the Alpine orogenies onto these sequences. The post-Variscan sandstones record Variscan cooling ages from (309.8±3.0 to 331.9±3.3 Ma), likewise indicating no Alpine thermal overprint. Consequently, the older source regions seem to have been nearly entirely eliminated during Variscan tectonic processes.

Acknowledgments: We acknowledge detailed reviews by Peter Árkai (Budapest) and Fritz Ebner (Leoben), which

helped to clarify presentation. We also acknowledge generous support by the Austrian Research Foundation FWF (Grant No. P10506-GEO) to FN. We thank Wolfgang Frisch (Tübingen), Konrad Hammerschmidt (Berlin), Christoph Heubeck (Berlin), and Igor Villa (Bern) for remarks on an initial version of the manuscript.

References

Aronson J.L. & Lewis T.L. 1994: Ages of detrital white mica from Devonian-Pennsylvanian strata of the North Central Appalachian basin: Dominance of the Acadian orogen as provenance. *J. Geol.* 102, 685–696.

Burghele A. 1987: Propagation of error and choice of standard in the ^{40}Ar-^{39}Ar technique. *Chem. Geol.* 66, 17–19.

Clauer N. 1981: Strontium and argon isotopes in naturally weathered biotites, muscovites and feldspars. *Chem. Geol.* 31, 325–334.

Copeland P. & Harrison T.M. 1990: Episodic rapid uplift in the Himalaya revealed by $^{40}Ar/^{39}Ar$ analysis of detrital K-feldspar and muscovite, Bengal Fan. *Geology* 18, 354–357.

Dallmeyer R.D. 1987: $^{40}Ar/^{39}Ar$ age of detrital muscovite within Lower Ordovician sandstone in the Coastal Plane basement of Florida: Implications for West African terrane linkages. *Geology* 15, 998–1001.

Dallmeyer R.D. & Nance R.D. 1990: $^{40}Ar/^{39}Ar$ ages of detrital muscovite within early Palaeozoic overstep sequences, Avalon composite terrane, southern New Brunswick: implications for extent of late Palaeozoic tectonothermal overprint. *Canad. J. Earth Sci.* 27, 1209–1214.

Dallmeyer R.D. & Neubauer F. 1994: Cadomian $^{40}Ar/^{39}Ar$ apparent age spectra of detrital muscovites from the Eastern Alps. *J. Geol. Soc. London* 151, 591–598.

Dallmeyer R.D. & Takasu A. 1992: $^{40}Ar/^{39}Ar$ ages of detrital muscovite and whole-rock slate/phyllite, Narragansett Basin, RI-MA, USA: implications for rejuvenation during very low-grade metamorphism. *Contr. Mineral. Petrology* 110, 515–527.

Fenninger A., Schönlaub H.P., Holzer H.-L. & Flajs G. 1976: Zu den Basisbildungen der Auernigschichten in den Karnischen Alpen (Österreich). *Verh. Geol. Bundesanst.* 1976, 243–255.

Fitch F.J., Miller J.A. & Tompson D.B. 1966: The palaeographic significance of isotopic age determinations on detrital micas from the Triassic of the Stockport-Macclesfield District, Chesire, England. *Palaeogeogr. Palaeoclimatol. Palaeoecol.* 2, 281–312.

Flisch M. 1982: Potassium-argon analysis. In: Odin G.S (Ed.): Numerical dating in stratigrapy. *Wiley, Sons,* Chichester–New York–Brisbane, 151–158.

Flügel H.W. 1975: Einige Probleme des Variszikums von Neo-Europa. *Geol. Rdsch.* 64, 1–62.

Frank W., Lelkes-Felvári G. & Dunkl I. 1996: Thermal history of Austroalpine basement rocks of the borehole Fertörákos-1004, Western Hungary. *Advances in Austrian-Hungarian Joint Geo. Res.,* Budapest 1996, 177–195.

Gradstein F.M., Ogg J.G., Smith A.G., Agterberg F.P., Bleeker W., Cooper R.A., Davydov V., Gibbard P., Hinnov L.A., House M.R., Lourens L., Luterbacher H.P., McArthur J., Melchin M.J., Robb L.J., Shergold J., Villeneuve M., Wardlaw B.R., Ali J., Brinkhuis H., Hilgen F.J., Hooker J., Howarth R.J., Knoll A.H., Laskar J., Monechi S., Plumb K.A., Powell J., Raffi I., Röhl U., Sadler P., Sanfilippo A., Schmitz B., Shackleton N.J., Shields G.A., Strauss H., Van Dam J., van Kolfschoten T., Veizer J. & Wilson D. 2004: A geologic time scale 2004. *Cambridge University Press*, 1–589.

Guidotti C.V. 1984: Micas in metamorphic rocks. In: Bailey S.W. (Ed.): Micas. *Rev. Mineralogy, Mineral. Soc. Amer.,* Washington D.C., 357–467.

Hames W.E. & Bowring S.A. 1994: An empirical evaluation of the argon diffusion geometry in muscovite. *Earth Planet. Sci. Lett.* 124, 161–167.

Handler R., Dallmeyer R.D. & Neubauer F. 1997: $^{40}Ar/^{39}Ar$ ages of detrital white mica from Upper Austroalpine units in the Eastern Alps, Austria: Evidence for Cadomian and contrasting Variscan sources. *Geol. Rdsch.* 86, 69–80.

Handler R., Dallmeyer R.D., Neubauer F. & Hermann S. 1999: $^{40}Ar/^{39}Ar$ mineral ages from the Kaintaleck Nappe, Austroalpine basement, Eastern Alps. *Geol. Carpathica* 50, 229–239.

Handler R., Velichkova S.H., Neubauer F. & Ivanov Z. 2004: $^{40}Ar/^{39}Ar$ age constraints on the timing of the formation of Cu-Au deposits in the Panagyurishte region, Bulgaria. *Schweiz. Mineral. Petrograph. Mitt.* 84, 1, 119–132.

Hodges K.V., Ruhl K.W., Wobus C.W. & Pringle M.S. 2005: $^{40}Ar/^{39}Ar$ thermochronology of detrital minerals. *Rev. Mineral. Geochem.* 58, 239–257.

Kelley S.P. & Bluck B.J. 1989: Detrital mineral ages from the Southern Uplands using ^{40}Ar-^{39}Ar laser probe. *J. Geol. Soc. London* 146, 401–403.

Kelley S.P. & Bluck B.J. 1992: Laser ^{40}Ar-^{39}Ar ages for individual detrital muscovites in the Southern Uplands of Scotland, U.K. *Chem. Geol., Isotope Geosci. Sect.* 101, 143–156.

Kirschner D.L., Cosca M.A., Masson H. & Hunziker J.C. 1996: Staircase $^{40}Ar/^{39}Ar$ spectra of fine-grained white mica: Timing and duration of deformation and empirical constraints on argon diffusion. *Geology* 24, 747–751.

Krainer K. 1993: Late- and Post-Variscan sediments of the Eastern and Southern Alps. In: von Raumer J.F. & Neubauer F. (Eds.): Pre-Mesozoic geology in the Alps. *Springer,* Heidelberg, 537–564.

Krylov A.Y. & Silin Y.I. 1959: Application of the argon method of age determination to the study of migration of terrigenous deposits. *Dokl. Akad. Nauk. SSSR* 129, 1069–1071.

Läufer A. 1996: Variscan and Alpine tectonometamorphic evolution of the Carnic Alps (Southern Alps) — structural analysis, illite crystallinity, K-Ar and Ar-Ar geochronology. *Tübinger Geowiss. Abh. A* 26, 1–102.

Läufer A.L., Frisch W., Steinitz G. & Loeschke J. 1997: Exhumed fault-bounded Alpine blocks along the Periadriatic lineament: the Eder unit (Carnic Alps, Austria). *Geol. Rdsch.* 86, 612–626.

Läufer A.L., Hubich D. & Loeschke J. 2001: Variscan geodynamic evolution of the Carnic Alps (Austria/Italy). *Int. J. Earth Sci.* 90, 855–870.

Mader D. & Neubauer F. 2004: Provenance of Palaeozoic sandstones from the Carnic Alps (Austria): petrographic and geochemical indicators. *Int. J. Earth Sci.* 93, 262–281.

McDougall I. & Harrison T.M. 1999: Geochronology and thermochronology by the $^{40}Ar/^{39}Ar$ method. *2nd edition, Oxford Monographs on Geology and Geophysics No. 9, Oxford University Press,* Oxford, 1–269.

Mitchell J.K. & Taka A.S. 1984: Potassium and argon loss patterns in weathered micas, implications for detrital mineral studies, with particular reference to the Triassic palaeography of the British Isles. *Sed. Geol.* 39, 27–52.

Müller W., Dallmeyer R.D., Neubauer F. & Thöni M. 1999: Deformation-induced resetting of Rb/Sr and $^{40}Ar/^{39}Ar$ mineral systems in a low-grade, polymetamorphic terrane (eastern Alps, Austria). *J. Geol. Soc. London* 156, 261–278.

Najman Y., Pringle M., Godin L. & Oliver G. 2001: Dating of the oldest continental sediments from the Himalayan foreland basin. *Nature* 410, 194–197.

Neubauer F. 1988: The Variscan orogeny in the Austroalpine and

Southalpine domains of the Eastern Alps. *Schweiz. Mineral. Petrogr. Mitt.* 68, 339-349.

Neubauer F. & Handler R. 1997: Mica tectonics. *Terra Nostra, Abstract, Jh. Geol. Vereinigung.*

Neubauer F. & Sassi F.P. 1993: The Austro-Alpine quartzphyllites and related Paleozoic Formations. In: von Raumer J.F. & Neubauer F. (Eds.): Pre-Mesozoic geology in the Alps. *Springer Verlag,* Berlin–Heidelberg, 423–439.

Neubauer F., Klötzli U. & Poscheschnik P. 2001: Cadomian magmatism in the Alps recorded in Late Ordovician sandstones of the Carnic Alps: preliminary results from zircon Pb/Pb evaporation dating. *Schweiz. Mineral. Petrogr. Mitt.* 81, 175–179.

Purdy J.W. & Jäger E. 1976: K-Ar ages on rock-forming minerals from the Central Alps. *Mem. Ist. Geol. Min. Univ. Padova* 30, 1–31.

Rantitsch G. 1997: Thermal history of the Carnic Alps (Southern Alps, Austria) and its palaeogeograhic implications. *Tectonophysics* 272, 213–232.

Renne P.R., Becker T.A. & Swapp S.M. 1990: $^{40}Ar/^{39}Ar$ laser probe dating of detrital micas from the Montgomery Creek Formation, northern California: Clues to provenance, tectonics, and weathering processes. *Geology* 18, 563–566.

Rieder M., Cavazzini G., D'Yakonov Y.S., Frank-Kamenetskij V.A., Gottardi G., Guggenheim S., Koval P.V., Muller G., Neiva A.M.R., Radoslovich E.W., Robert J.L., Sassi F.P., Takeda H., Weiss Z. & Wones D.R. 1998: Nomenclature of the micas. *Amer. Mineral.* 83 (11–12 Part 1), 1366 (online, 1–8).

Robbins C.S. 1972: Radiogenic argon diffusion in muscovite under hydrothermal conditions. Unpubl. *MSc Thesis, Brown Univ.,* Providence R.I., 1–88.

Schönlaub H.P. 1985a: Das Paläozoikum der Karnischen Alpen. *Arbeitstagung Geol. Bundesanst., Kötschach-Mauthen, Gailtal, Geol. Bundesanst.,* Wien, 52–54.

Schönlaub H.P. 1985b: Geologische Karte der Republik Österreich 1:50,000, 197 Kötschach. *Geol. Bundesanst.,* Wien.

Schönlaub H.P. 1987: Geologische Karte der Republik Österreich 1:50,000, 198 Weissbriach. *Geol. Bundesanst.,* Wien.

Schönlaub H.P. & Heinisch H. 1993: The classic fossiliferous Paleozoic units of the Eastern Alps. In: von Raumer J.F. & Neubauer F. (Eds.): Pre-Mesozoic geology in the Alps. *Springer,* Berlin–Heidelberg–New York, 395–422.

Schönlaub H.P. & Histon K. 2000: The Paleozoic evolution of the Southern Alps. *Mitt. Österr. Geol. Gesell.* 92, 1999, 15–34.

Sherlock S.C., Jones K.A. & Jones J.A. 2000: A central European Variscide source for Upper Carboniferous sediments in SW England; $^{40}Ar/^{39}Ar$ detrital white mica ages from the Forest of Dean Basin. *J. Geol. Soc. London* 157, 905–908.

Sonntag A., Bracke G., Loeschke J. & Satir M. 1997: Untersuchungen an Zirkonen aus dem Flysch der Karawanken: Ihre Bedeutung für potentielle Liefergebiete und paläogeographische Fragen. *Jb. Geol. Bundesanst.* 140, 2, 251–273.

Spaletta C., Vai G.B. & Venturini C. 1980: The Hercynian flysch of Paularo and Dimon Mountains (Carnic Alps). *Mem. Soc. Geol. Ital.* 20, 243–265 (in Italian).

Spear F.S. 1993: Metamorphic phase equilibria and pressure-temperature-time paths. *Mineral. Soc. Amer.,* Washington D.C., 1–799.

Speer J.A. 1984: Micas in igneous rocks. In: Bailey S.W. (Ed.): Micas. *Rev. Mineral., Mineral. Soc. Amer., Washington D.C.* 299–356.

Steiger R.H. & Jäger E. 1977: Subcommission on geochronology: Convention on the use of decay constants in geo- and cosmochronology. *Earth Planet. Sci. Lett.* 36, 359–362.

Tollmann A. 1985: Der südalpine Anteil Österreichs. *Geol. Österreich, Band 2, Außerzentralalpiner Anteil, Deuticke,* Wien, 240–300.

Villa I. 1998: Isotopic closure. *Terra Nova* 10, 42–47.

Vistelius A.B. 1959: The problem of the origin of the red beds of Cheleken Peninsula, an experiment on the use of absolute age of clastic minerals for the solution of problems of lithology and paleogeography. *Dok. Akad. Nauk. SSSR* 125, 483–486.

von Blanckenburg F., Villa I.M., Baur H., Morteani G. & Steiger R.H. 1989: Time calibration of a P-T path from the western Tauern Window, Eastern Alps: The problem of the closure temperatures. *Contr. Mineral. Petrology* 101, 1–11.

von Eynatten H., Schlunegger F., Gaupp R. & Wijbrans J.R. 1999: Exhumation of the Central Alps: evidence from $^{40}Ar/^{39}Ar$ laserprobe dating of detrital white micas from the Swiss Molasse Basin. *Terra Nova* 11, 284–289.

Vozárová A., Frank W., Král J. & Vozár J. 2005: $^{40}Ar/^{39}Ar$ dating of detrital mica from the Upper Paleozoic sandstones in the Western Carpathians (Slovakia). *Geol. Carpathica* 56, 463–472.

Welzel B. 1991: Die Bedeutung von K/Ar-Datierungen an detritischen Muskoviten für die Rekonstruktion tektonometamorpher Einheiten im Liefergebiet — ein Beitrag zur Frage der varistischen Krustenentwicklung in der Böhmischen Masse. *Gött. Arbeit. Geol. Paläont.* 49, 1–61.